The Structures and Reactions of Linear and Cyclic C_6 Hydrocarbons Adsorbed on the Pt(111) Crystal Surface Studied by Sum Frequency Generation Vibrational Spectroscopy: Pressure, Temperature, and H_2 Coadsorption Effects†

Minchul Yang, Keng C. Chou, and Gabor A. Somorjai*

Department of Chemistry, University of California, Berkeley, California 94720, and Materials Science Division, Lawrence Berkeley National Laboratory, Berkeley, California 94720

Received: April 22, 2004; In Final Form: June 13, 2004

We studied the adsorption structures and reactions of C_6 hydrocarbon molecules (cyclohexene, cyclohexane, 1-methylcyclohexene, *n*-hexane, 2- and 3-methylpentanes, and 1-hexene) on Pt(111) using sum frequency generation (SFG) vibrational spectroscopy. The experiments were performed in the presence and absence of excess hydrogen and as a function of temperature. Upon cyclohexene adsorption on Pt(111) at 1.5 Torr, 1,3- and 1,4-cyclohexadienes and π-allyl C_6H_9 were observed in the presence of excess hydrogen. Cyclohexane adsorption at 1.5 Torr resulted in the formation of cyclohexyl on the surface in the presence of excess hydrogen but π-allyl C_6H_9 in absence of excess hydrogen. 1-Methylcyclohexene formed methylcyclohexenyl on the surface only in the presence of excess hydrogen. *n*-Hexane and 3-methylpentane adsorbed molecularly on Pt(111) at 296 K in the presence of excess hydrogen. 2-Methylpentane and 1-hexene were readily dehydrogenated to form metallacyclobutane and hexylidyne even at 296 K, regardless of the presence of excess hydrogen. *n*-Hexane was dehydrogenated to form hexylidyne or metallacyclic species at high temperature in the presence of excess hydrogen. Hexylidyne and metallacyclic species were also main surface intermediates in dehydrogenation of 2- and 3-methylpentane. The absence of excess hydrogen induced dehydrocyclization of *n*-hexane to form π-allyl c-C_6H_9. On the basis of the SFG results, the mechanism of the *n*-hexane conversion to benzene is discussed.

1. Introduction

The chemistry of C_6 linear and cyclic hydrocarbons on platinum surfaces is of special interest for those aiming to understand the "reforming" reactions that produce high-octane gasoline.[1,2] Model reaction studies use *n*-hexane or *n*-heptane as the starting molecule that is converted to branched isomers or aromatics. Several reaction intermediates have been identified, including 1-hexene, cyclohexane, cyclohexene, and methylcyclopentane. These molecules are then converted to the desired end products, such as 2- and 3-methylpentanes and benzene or substituted benzene. The reactions are usually carried out in excess hydrogen and at high pressures and temperatures.[1−3]

Catalytic reactions of *n*-hexane on Pt-based catalysts in the presence of excess hydrogen include, in general, four classes of reactions: (a) dehydrocylization to form benzene, (b) cyclization to form methylcyclopentane, (c) isomerization to form 2- and 3-methylpentane, and (d) hydrogenolysis to form smaller hydrocarbons.[2,4] It has been suggested that dehydrocylization occurs via direct 1,6-ring closure rather than ring enlargement of methylcyclopentane.[4] Direct 1,6-ring closure can take place via two different pathways. One is consecutive dehydrogenation of *n*-hexane to hexene−hexadiene−hexatriene followed by cyclization.[2,4,5] The other is the formation of cyclohexane followed by its consecutive dehydrogenation to cyclohexene−cyclohexadiene−benzene.[6] On the other hand, isomerization of *n*-hexane is believed to occur via formation of methylcyclopentane followed by hydrogenolysis to form 2- and 3-methylpentane.[2] Although enormous progress has been made in studies of the reaction kinetics, functionality of active sites, and structural sensitivity, a detailed understanding of elementary reaction steps and reactive surface intermediates in the reaction steps still remains to be achieved.

To explore the elementary steps in this complex sequence of reactions, we have investigated the surface structures of the reactant and product molecules, and the most probable reaction intermediates of these reactions on the Pt(111) single-crystal surface. These experiments were performed at high reactant pressures (∼1.5 Torr), in the presence and absence of excess hydrogen, and as a function of temperature. We use sum frequency generation (SFG) vibrational spectroscopy for this purpose. This nonlinear optical technique can be employed at high pressures, and it is uniquely surface-sensitive because of the selection rules originating from the second-order optical process.[7−9] The second-order optical process is allowed only in a medium with no inversion symmetry. Because inversion symmetry is always broken at interfaces, the SFG technique is capable of observing vibrational spectra of molecules adsorbed on surfaces.

We find that all of the molecules form dehydrogenated species even in the presence of excess hydrogen. For example, cyclohexene (C_6H_{10}) forms cyclohexenyl (C_6H_9) on the platinum surface. Cyclohexane (C_6H_{12}) forms cyclohexyl (C_6H_{11}). *n*-Hexane (C_6H_{14}) and 1-hexene (C_6H_{12}) form hexylidyne (C_6H_{11}). These species have characteristic vibrational signatures. De-

* To whom correspondence should be addressed. Tel.: 510-642-4053. Fax: 510-643-9668. E-mail: somorjai@socrates.berkeley.edu.

† Part of the special issue "Gerhard Ertl Festschrift".

10.1021/jp048238n CCC: $27.50
Published on Web 07/28/2004

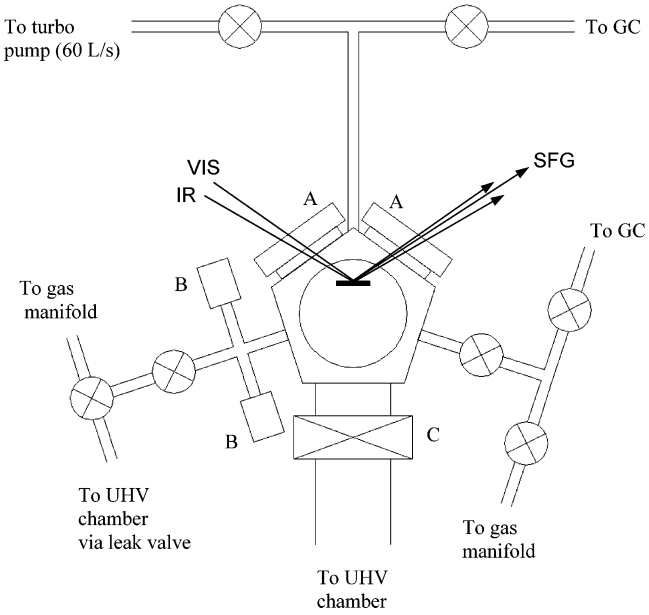

Figure 1. Schematic diagram of the high-pressure (HP) reaction cell. The system is composed of two CaF_2 windows (A), two pressure gauges (B), and a gate valve (C). Two gas lines from the HP cell are connected to a gas chromatograph (GC). Another gas line from the HP cell is connected to the UHV chamber via a leak valve. The HP cell contains two separate gas lines to introduce two different gases simultaneously. Directions of visible (VIS), infrared (IR), and SFG beams are also illustrated.

pending on hydrogen pressure, *n*-hexane either forms the linear hexylidyne or the cyclic cyclohexenyl on the surface. The former produces branched isomers, whereas the latter forms benzene. In this paper, we discuss temperature- and excess-hydrogen-dependent surface chemistry of the linear and cyclic C_6 hydrocarbons.

2. Experimental Section

2.1. High-Pressure/Ultrahigh-Vacuum (HP/UHV) System. All experiments were carried out on a Pt(111) single-crystal surface in a high-pressure/ultrahigh-vacuum (HP/UHV) system. The HP/UHV system consists of an HP cell, a UHV chamber, and a magnetically coupled sample transporter. The UHV chamber is equipped with an Auger electron spectrometer (AES) and a quadrupole mass spectrometer (QMS). The chamber can be pumped to a base pressure of 3×10^{-10} Torr. The HP cell, where high-pressure catalysis studies were carried out, is connected to the UHV chamber through a gate valve. A sample transfer arm is connected to the UHV chamber at 180° to the HP reaction cell such that a sample can be transferred between the UHV chamber and the HP cell along a horizontal linear path.

The HP cell, which is a 600-mL stainless steel cell electroplated with gold to reduce catalytic reactivity, is equipped with several ports (Figure 1). Two CaF_2 conflat windows (A) are attached at an angle of 120° with respect to each other on the HP cell, allowing input and output of infrared (IR) and visible (VIS) beams for SFG experiments. Two gas lines from the HP cell are connected to a gas chromatograph (GC) for monitoring of reaction kinetics. Another gas line from the HP cell is connected to the UHV chamber for monitoring partial pressures of gas products during reactions using the QMS. The HP cell contains two separate gas lines, allowing for the introduction of two different gases simultaneously. The operating pressure of the HP cell is measured with two attached capacitance manometers, for pressure ranges between 0.1 and 1000 mTorr and between 0.1 and 1000 Torr. The HP cell can be independently pumped by a turbo pump, allowing rapid evacuation of high-pressure gases after completion of a reaction. The HP cell was equipped with a reaction loop that contained a recirculation pump and septum for gas abstraction and GC analysis. For GC measurements using packed columns (Alltech), the reactant and product gases in the HP cell were constantly mixed by a recirculation pump. Periodic sampling allowed kinetic measurements of the gas-phase composition.

The Pt(111) crystal was cleaned by sputtering with Ar^+ ions (1 keV), heating at 900 K in the presence of 5×10^{-7} Torr O_2 for 2 min, and then annealing at 1200 K in UHV for 2 min. After a few cycles of cleaning, the Pt(111) crystal was transferred to the HP cell for SFG and GC measurements. The Pt(111) surface was routinely checked by AES for cleanliness. All samples were purified by several freeze−pump−thaw cycles before being introduced in the HP cell. The reactant pressure was normally 1.5 Torr of C_6 hydrocarbon or 1.5 Torr of C_6 hydrocarbon and 15 Torr of hydrogen.

2.2. Sum Frequency Generation (SFG) Vibrational Spectroscopy: Experimental Setup and Theory. The SFG measurements were performed using a Nd:YAG laser at 1064 nm with a 20-ps pulse width and a 20-Hz repetition rate. The 1064-nm beam was frequency-doubled to 532 nm in a $KTiOPO_4$ (KTP) crystal. The tunable IR beam was generated in an $AgGaS_2$ crystal by difference frequency mixing of the 1064-nm beam with the output of a β-BaB_2O_4 (BBO) optical parametric generator/amplifier (OPG/OPA) pumped by the 532-nm beam. The VIS beam (200 μJ/pulse) and the IR (100 μJ/pulse) beam were spatially and temporally overlapped on the Pt(111) surface with incident angles of 55° and 60° , respectively, with respect to the surface normal. All spectra were taken using a ppp polarization combination (p-polarized for the SFG, VIS, and IR beams). As the IR beam was scanned over the frequency range of interest, the sum frequency output from the Pt(111) crystal was collected by a photomultiplier and a gated integrator.

The theory of SFG for surface studies has been described in detail previously.[7−9] Briefly, SFG is a second-order nonlinear optical process in which an infrared laser beam at ω_{IR} is combined with a visible laser beam at ω_{VIS} to generate a sum frequency output at $\omega_{SF} = \omega_{IR} + \omega_{VIS}$. This process is only allowed in a medium without centrosymmetry under the electric dipole approximation. Platinum bulk is centrosymmetric, and its contribution to SFG is usually negligible. Isotropic gases in the HP cell do not generate SFG. Only the metal surface and adsorbates on the surface can generate SFG under the electric dipole approximation. The SFG signal, I_{SF}, is related to the incidence visible (I_{VIS}) and infrared (I_{IR}) beam intensities and second-order susceptibility of the media ($\chi^{(2)}$) as

$$I_{SF} \propto |\chi^{(2)}|^2 I_{VIS} I_{IR} \tag{1}$$

The second-order susceptibility $\chi^{(2)}$ is given by

$$\chi^{(2)} = \chi_{NR} + \sum_q \frac{A_q}{\omega_{IR} - \omega_q + i\Gamma_q} \tag{2}$$

where χ_{NR} is the nonresonance contribution, and A_q, ω_q, and Γ_q denote the vibrational mode strength, the resonant frequency, and the line width of the q_{th} vibrational mode, respectively. The nonresonance contribution, χ_{NR}, originates from the metal surface and is usually independent of the frequency of the

infrared laser beam. In contrast, the second term is significantly enhanced when the frequency of the infrared laser beam is in resonance with a vibrational mode of the adsorbates. The vibrational mode strength A_q is given by[10]

$$A_{q,ijk} = \frac{2\pi}{h} N \langle \sum_{lmn} F_{q,ijk} (\hat{i}\cdot\hat{l})(\hat{j}\cdot\hat{m})(\hat{k}\cdot\hat{n}) R_{q,lm} \mu_{q,n} \rangle \qquad (3)$$

where N is the number density of adsorbates; $F_{q,ijk}$ is the Fresnel factor; and $R_{q,lm}$ and $\mu_{q,n}$ are the Raman and the IR transition cross sections, respectively, for the q_{th} vibrational mode. i, j, and k refer to the laboratory coordinates, and l, m, and n refer to the molecular coordinates. The brackets indicate the spatial average of the molecular orientations. Because the Fresnel factor is complex, A_q can be expressed as $A_q = |A_q|e^{i\phi_q}$ where ϕ_q is the phase factor. χ_{NR} is also complex, given as $\chi_{\text{NR}} = |\chi_{\text{NR}}|e^{i\varphi}$. Finally, the SFG signal is written as

$$I_{\text{SF}} \propto \left| |\chi_{\text{NR}}| e^{i\varphi} + \sum_q \frac{|A_q| e^{i\phi_q}}{\omega_{\text{IR}} - \omega_q + i\Gamma_q} \right|^2 I_{\text{VIS}} I_{\text{IR}} \qquad (4)$$

The relative SFG peak intensities between the vibrational modes are useful for evaluating the molecular orientations of surface species because the Raman and the IR transition cross sections are sensitive to the molecular orientations.[11,12] The quantitative analysis of SFG spectra requires a detailed understanding of both the IR and Raman transitions of the molecule on the surface. The interferences between the nonresonance and resonance contribution should also be considered for quantitative analysis of SFG spectra. The surface IR spectra for interesting molecules on Pt(111) are abundant in the literature,[13,14] whereas their Raman spectra are scarce because of low Raman scattering cross sections of adsorbates on flat metal surfaces. In these circumstances, the interpretation of our SFG spectra will be based on the surface IR spectra in the literature. This approach was found to be valid for gaining some insight into the molecular orientations (but only for qualitative purpose). The reasons are as follows. The SFG spectrum from the adsorbates on the metal surface should obey the IR surface selection rule that only the IR transition dipole vector component perpendicular to the metal surface accounts for the IR transition cross sections. Moreover, the classical theory of the Raman surface selection rule predicts that the Raman band intensity should scale as $\alpha(z^2) > \alpha(xy)$, $\alpha(yz) \gg (\alpha x^2)$, $\alpha(y^2)$, $\alpha(xy)$, where α is the Raman scattering tensor element; x, y, and z refer to the laboratory coordinates; and z is the axis along the surface normal.[15,16] This means that both the IR and Raman transition cross sections are sensitive to the molecular orientation with respect to the surface normal and so, therefore, is the SFG intensity. Moreover, the nonresonant SFG signal from a Pt surface is much smaller than that from other metal surfaces such as Au and Ag.

To analyze our SFG spectra, the SFG signal was first normalized to the intensity (I_{IR}) of the incident infrared beam on the surface. This is necessary because gas molecules in the HP cell absorb some portion of the incident infrared beam. Detailed descriptions on the HP/UHV system and SFG measurement can be found elsewhere.[17,18]

3. Results and Discussion

The SFG results for the C_6 hydrocarbons are described in the order of C_6 cyclic hydrocarbons (cyclohexene, cyclohexane, and 1-methylcycloehxene) and C_6 linear hydrocarbons (*n*-hexane, 3-methylpentane, 2-methylpentane, and 1-hexene).

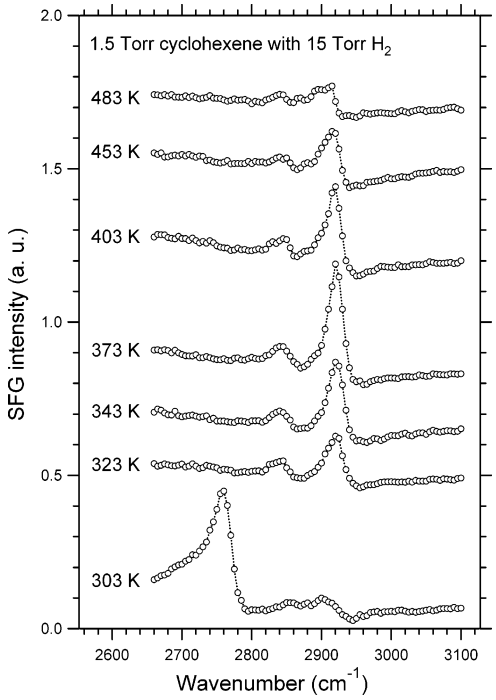

Figure 2. Temperature-dependent SFG spectra of surface species on Pt(111) under 1.5 Torr of cyclohexene and 15 Torr of H_2 in the range of 303−483 K. Dotted lines are drawn for visual aides.

Cyclohexene was chosen as the starting molecule because cyclohexene adsorption on Pt(111) is the most extensively studied in UHV conditions. In addition, the vibrational spectra of the surface species upon cyclohexene adsorption on Pt(111) are relatively simple: they involve only CH_2 modes in the CH stretching region at 2800−3000 cm^{-1}.

The SFG experiments were performed at various temperatures and pressures in the presence and absence of excess hydrogen. Effects of excess hydrogen on the structure and reaction of the hydrocarbons are of special interest because many hydrocarbon catalytic reactions are carried out in the presence of excess hydrogen.[1]

3.1. Adsorption Structure and Reactions of Cyclohexene on Pt(111). *Temperature Dependence of Surface Species under 1.5 Torr of Cyclohexene and 15 Torr of H_2.* The temperature-dependent SFG spectra of surface species on Pt(111) under 1.5 Torr of cyclohexene and 15 Torr of H_2 are shown in Figure 2. The metal surface was initially kept at 303 K and then heated sequentially for each SFG measurement. The dominant band at 2760 cm^{-1} at 303 K is assigned to the C−H stretch from 1,4-cyclohexadiene. The red shift from the typical CH_2 stretching range (2840−2940 cm^{-1}) is due to strong electron donation from the C−H bond to the platinum surface.[19] The three discernible bands at 2855, 2880, and 2900 cm^{-1} are characteristics of 1,3-cyclohexadiene adsorbed on Pt(111).[20−22] At 323 K, the band at 2760 cm^{-1} completely disappears, and two new bands appear at 2840 and 2920 cm^{-1}. The bands at 2840 and 2920 cm^{-1} are typical of symmetric and asymmetric C−H stretches, respectively, of a CH_2 group. The band positions and their relative intensities are consistent with those of π-allyl c-C_6H_9.[23] The proposed molecular structures of 1,3- and 1,4-cyclohexadienes and π-allyl c-C_6H_9 are illustrated in Scheme 1. Above 403 K, two additional bands grow at 2870 and 2900 cm^{-1}, becoming more discernible at 483 K. The SFG bands in the range of 2800−3000 cm^{-1} at 483 K are assigned to C−H stretches of 1,3-cyclohexadiene.

SCHEME 1

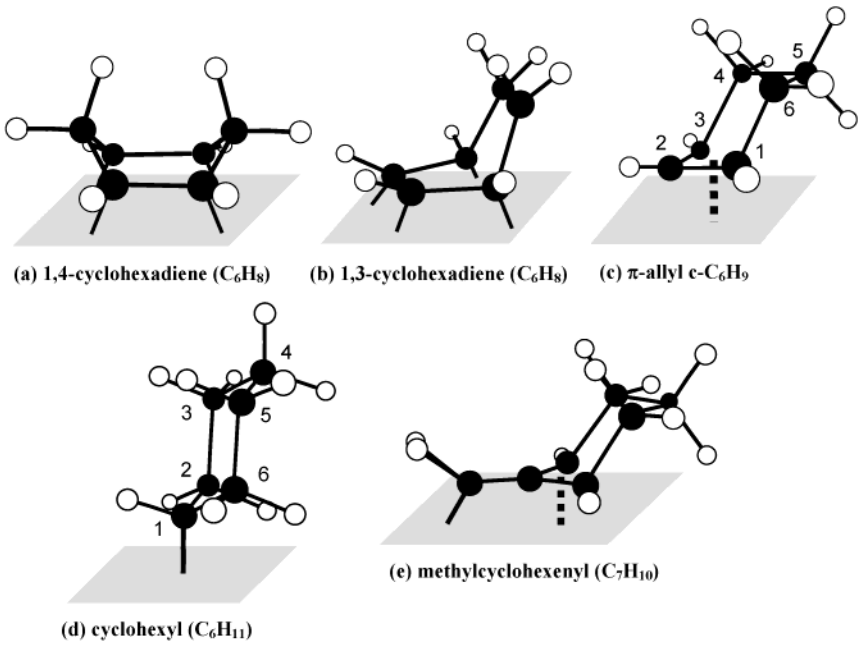

Cyclohexene adsorption on Pt(111) at low pressures ($<10^{-6}$ Torr) has been studied using various surface analytical techniques, such as thermal desorption spectroscopy (TDS),[24] bismuth postdosing TDS (BPTDS),[24,25] laser-induced thermal desorption (LITD),[26] high-resolution electron-energy loss spectroscopy (HREELS),[26,27] and reflection−absorption IR spectroscopy (RAIRS).[22] Briefly, cyclohexene exists in a di-σ form on Pt(111) at 100 K. It converts to π-allyl c-C_6H_9 at about 200 K.[22,25] At about 300 K, π-allyl c-C_6H_9 converts to benzene. Further heating induces desorption and decomposition of benzene.[22,25,26] The observed surface species at various temperatures are summarized in Scheme 1. As seen in Scheme 1, the conversion temperature of cyclohexene to π-allyl c-C_6H_9 at high pressure is higher than that at low pressure by about 100 K. This is probably due to a site-blocking effect of high-coverage surface species at high pressure of cyclohexene. It is known that dehydrogenation processes require free active sites for C−H bond cleavage. High-coverage surface species block active sites for the C−H bond cleavage, inhibiting dehydrogenation. The site-blocking effect has been observed for dehydrogenation of cyclic hydrocarbons.[28,29]

The observation of 1,3-cyclohexadiene over 400 K exemplifies the difference in chemical environments on the surface under low-pressure ($<10^{-6}$ Torr) and high-pressure (>1 Torr) conditions. At low pressure, none of the intermediates with stoichiometries between C_6H_9 and benzene, such as C_6H_8 and C_6H_7, has been observed in the process of dehydrogenation of cyclohexane (or cyclohexene) to benzene.[22,25−27] This can be understood by considering the thermochemistry of these intermediates on Pt(111). According to semiempirical thermodynamic calculations by Koel et al.,[30] a C−H cleavage from π-allyl c-C_6H_9 is a slow step with an activation energy of 22 kcal/mol for benzene formation on the surface. Once 1,3-cyclohexadiene (C_6H_8) is formed from π-allyl c-C_6H_9, only 7 kcal/mol is necessary for further dehydrogenation to benzene on the surface. Therefore the surface coverage of C_6H_8 and C_6H_7 should be much lower than those of π-allyl c-C_6H_9 and benzene. High-pressure conditions allow one to observe such a metastable reactive intermediate as 1,3-cyclohexadiene. This unique capability of SFG in observing low-coverage reactive intermediates has been previously demonstrated by Cremer et al.[31] Their SFG results showed that π-bonded ethylene with a coverage of 0.04 ML (ML = monolayer) exists on Pt(111) during hydrogenation of 35 Torr ethylene at 295 K.[31] In UHV environments, by contrast, π-bonded ethylene exists only below 52 K.[32] Moreover, the π-bonded ethylene has proven to be the primary intermediate in the high-pressure ethylene hydrogenation on Pt(111).[31]

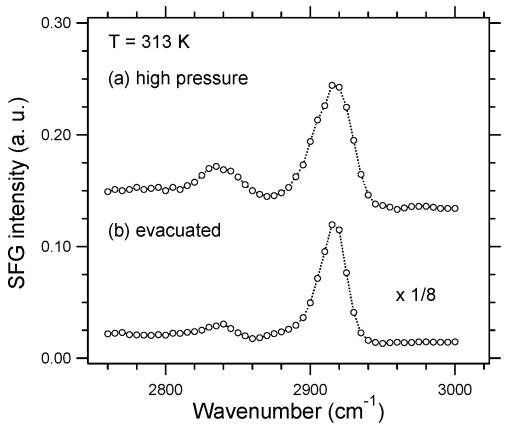

Figure 3. SFG spectra at 313 K taken (a) under 1.5 Torr of cyclohexene and 15 Torr of H_2 and (b) after evacuation.

Hydrogen Effect on Surface Species under 1.5 Torr of Cyclohexene at 313 K. The effect of excess hydrogen on the surface species was studied by comparing the SFG spectra before and after evacuating the HP cell. Figure 3a shows the SFG spectrum at 313 K under 1.5 Torr of cyclohexene and 15 Torr of H_2, and Figure 3b shows the SFG spectrum taken after the HP cell is quickly evacuated below 5×10^{-9} Torr. Because the associative desorption energy of H_2 on Pt(111) is only 9.4 kcal/mol,[33] the surface coverage of hydrogen is negligible at 313 K and below 5×10^{-9} Torr, giving rise to a hydrogen-deficient surface. The SFG spectrum in Figure 3b is consistent with that in Figure 3a in terms of the peak positions and their relative intensities, indicating that π-allyl c-C_6H_9 remained stable on the hydrogen-deficient surface after evacuation. The main difference is that the SFG bands of the C_6H_9 in Figure 3a are broader than those in Figure 3b, and their intensities are about an order of magnitude lower than those in Figure 3b.

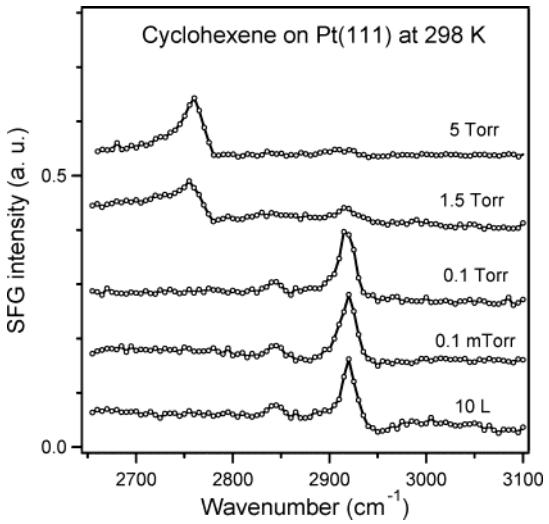

Figure 4. SFG spectra of surface species on Pt(111) at 298 K at various pressures of cyclohexene: 10 L and 10^{-4}, 0.1, 1.5, and 5 Torr, from the bottom. For an exposure of 10 L, cyclohexene was dosed for 100 s at 1×10^{-7} Torr.

The band broadening in the SFG spectrum is a result of the increase in the degree of disordering of π-allyl c-C_6H_9 on the surface. When the surface species is more disordered on the surface, there exist multiple chemisorption sites and intermolecular interactions, giving rise to inhomogeneous broadening of the SFG spectra. The increased disordering of π-allyl c-C_6H_9 could be one of the reasons for the intensity decrease of the SFG bands in the presence of excess H_2 as well. This is because SFG is a coherent process.[8] Another possible reason for the intensity change is the reduction of the surface coverage of π-allyl c-C_6H_9. Excess hydrogen on the surface might increase the conversion rate of π-allyl c-C_6H_9 to cyclohexene (C_6H_{10}) or cyclohexane (C_6H_{12}) that will quickly desorb from the surface. In summary, excess hydrogen increases the disordering and/or decreases the surface coverage of π-allyl c-C_6H_9 on Pt(111). Both cases appear to be associated with the C_6H_9−Pt bond weakening by excess hydrogen. A similar hydrogen effect was reported for cyclohexane adsorption on hydrogen-preadsorbed Pt(111).[34,35] In this case, preadsorbed hydrogen lowered the onset temperature of molecular desorption of cyclohexane by weakening the cyclohexane−Pt bond.

Influence of Cyclohexene Pressure on Surface Species and Reaction Pathways in the Absence of Excess Hydrogen: Stepwise Hydrogenation/Dehydrogenation vs Disproportionation. The pressure dependence of the major surface species was studied for cyclohexene adsorption on Pt(111) in the absence of excess hydrogen. Figure 4 shows the SFG spectra of surface species on Pt(111) at 298 K at various pressures of cyclohexene. At an exposure of 10 Langmuir (L, 1 L = 10^{-6} Torr s), the SFG spectrum features two major bands at 2845 and 2920 cm^{-1} that are assigned to π-allyl C_6H_9. The two bands remain unchanged as the cyclohexene pressure is increased up to 0.1 Torr, but disappear almost completely at 1.5 Torr. At 1.5 Torr, a new band appears at 2755 cm^{-1} that is assigned to 1,4-cyclohexadiene. The observation of π-allyl c-C_6H_9 as a major surface species at 298 K is consistent with previously reported results on cyclohexene adsorption on Pt(111) at submonolayer coverages.

As the pressure of cyclohexene increases, a new reaction channel becomes accessible: bimolecular reactions between surface intermediates and excess cyclohexene reactant. It is well-known that catalytic hydrogen-atom-transfer reactions between

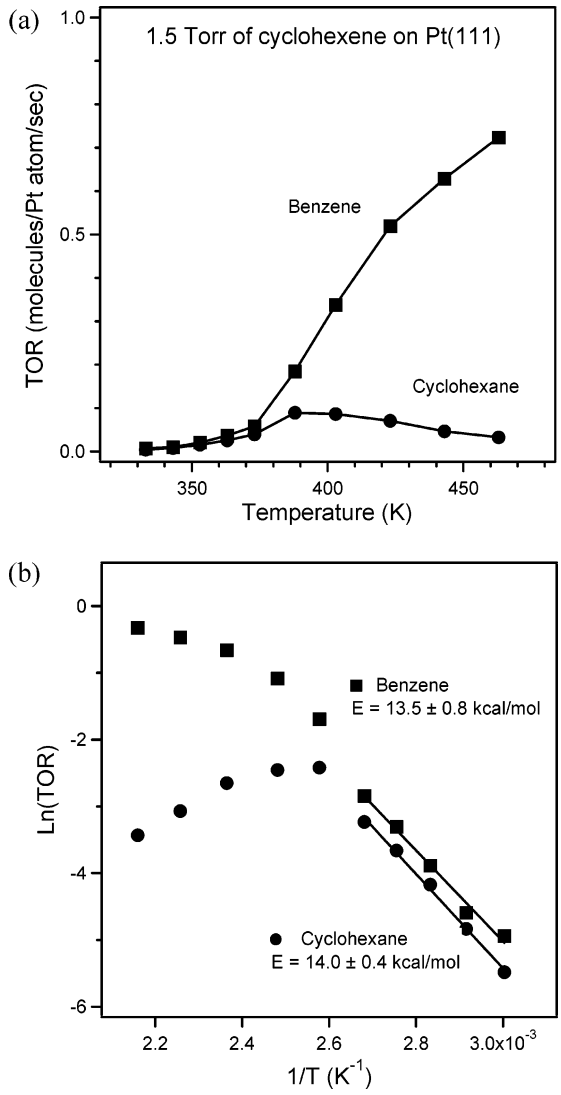

Figure 5. (a) Turnover rates (TORs), in molecules per Pt atom per second, for cyclohexene (at 1.5 Torr) catalytic reactions to form cyclohexane and benzene and (b) Arrhenius plots of the TORs. Apparent activation energies are 14.0 ± 0.4 kcal/mol for cyclohexane production and 13.5 ± 0.8 kcal/mol for benzene production.

cycloalkenes and many organic molecules are facile on Pd- or Pt-based catalysts even at room temperature.[36−38] In particular, cyclohexene and cyclohexadienes serve as some of most efficient hydrogen donor molecules in various bimolecular reactions occurring on heterogeneous catalysts.[36,37,39,40] Cyclohexene and cyclohexadienes are also readily hydrogenated on Pt(111) in the presence of excess hydrogen to form cyclohexyl (C_6H_{11}) and C_6H_9, respectively, which requires no activation energy.[30] The unique capability of the C_6 cyclic hydrocarbons as a hydrogen donor and acceptor accounts for disproportionation of cyclohexene, in which three cyclohexene molecules are involved to produce one benzene and two cyclohexane molecules.

Evidence of cyclohexene disproportionation was provided from the kinetics studies under 1.5 Torr of cyclohexene in the absence of excess hydrogen. Figure 5a shows the initial turnover rates (TORs), in molecules per Pt atom per second, for the cyclohexane and benzene productions as a function of temperature at 330−470 K. Figure 5b shows Arrhenius plots for the TORs. Apparent activation energies obtained in the temperature range 333−373 K were 14.0 ± 0.4 kcal/mol for cyclohexane and 13.5 ± 0.8 kcal/mol for benzene. The production of

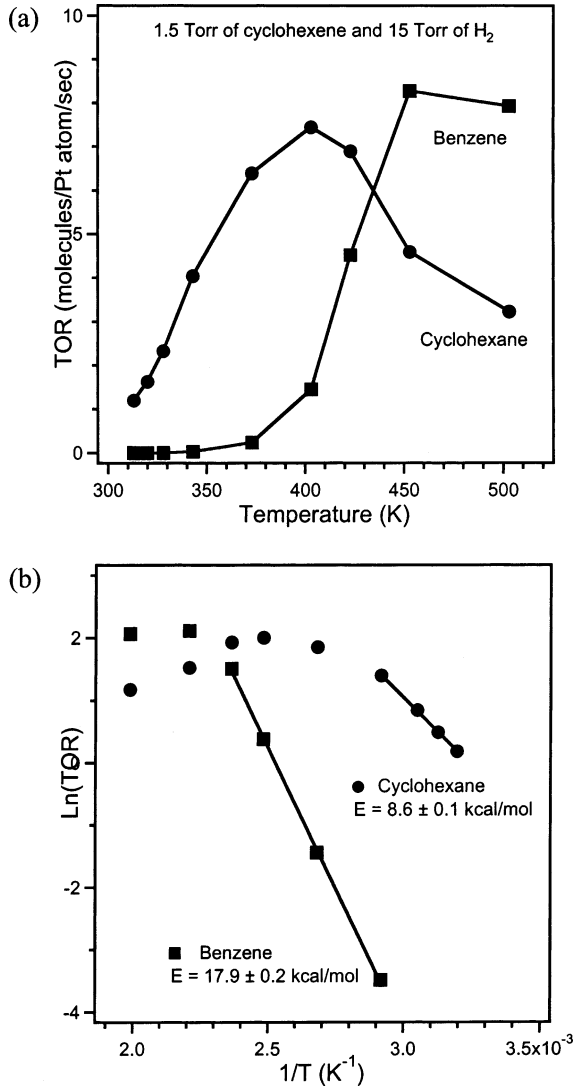

Figure 6. (a) Turnover rates (TORs) of cyclohexane and benzene productions under 1.5 Torr of cyclohexene and 15 Torr of H_2 and (b) Arrhenius plots of the TORs. Apparent activation energies are 8.6 ± 0.1 kcal/mol for cyclohexane production and 17.9 ± 0.2 kcal/mol for benzene production.

cyclohexane resulted from disproportionation rather than stepwise hydrogenation because the surface was hydrogen-deficient in these experiments. Moreover, the equivalence of the apparent activation energies for the two products within the uncertainty limit implies that the cyclohexane and benzene productions took place through the same reaction pathway.

A dramatic change in the reaction pathways due to excess hydrogen is demonstrated in Figure 6, which shows the temperature dependence of the TORs under 1.5 Torr of cyclohexene and 15 Torr of H_2 over Pt(111). Apparent activation energies are 8.6 ± 0.1 kcal/mol for cyclohexane and 17.9 ± 0.2 kcal/mol for benzene. In summary, in the absence of excess hydrogen, both cyclohexane and benzene are produced via disproportionation with apparent activation energies of about 14 kcal/mol. In the presence of excess hydrogen, cyclohexane is produced via stepwise hydrogenation with an activation energy of 8.6 kcal/mol, and benzene is produced via stepwise dehydrogenation with an activation energy of 17.9 kcal/mol.

3.2. Adsorption Structure and Reactions of Cyclohexane on Pt(111). *Temperature Dependence of Surface Species under 1.5 Torr of Cyclohexane and 15 Torr of H_2.* The temperature-dependent SFG spectra of surface species on Pt(111) under 1.5

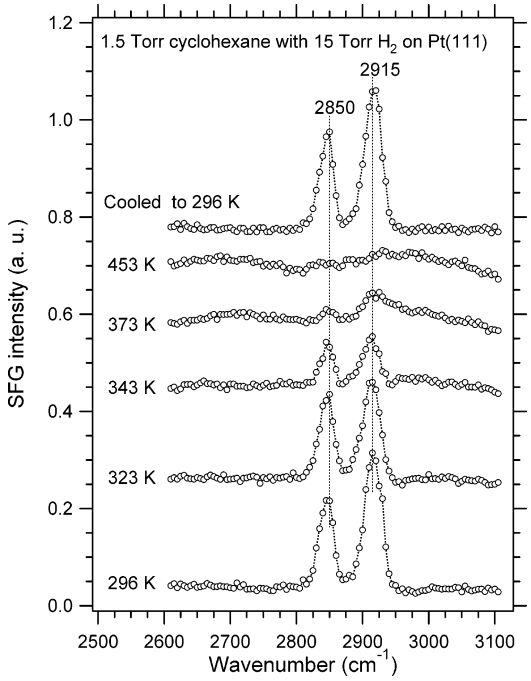

Figure 7. Temperature-dependent SFG spectra of cyclohexyl on Pt(111) under 1.5 Torr of cyclohexene and 15 Torr of H_2 in the temperature range of 296−453 K. The metal surface was initially kept at 296 K and then heated sequentially for each SFG measurement. The SFG spectrum at the top was taken after the metal surface was cooled to 296 K.

Torr of cyclohexane and 15 Torr of H_2 are shown in Figure 7. As temperature increases, the SFG bands decay in intensity, becoming featureless at 453 K. The SFG spectrum changes reversibly in the temperature range of 296−453 K. The SFG spectrum at the top in Figure 3 was obtained after the metal surface was cooled from 453 to 296 K. The SFG spectrum after the sample had been cooled is very similar to that at 296 K before the sample was heated. The two bands shown at 2850 and 2915 cm^{-1} are assigned to symmetric and asymmetric C−H stretch of a methylene group from a cyclohexyl (C_6H_{11}) intermediate (Scheme 1). The fact that the band positions do not change with temperature indicates that cyclohexyl does not undergo dehydrogenation in this temperature range. It should be noted that the SFG spectrum in Figure 7 is different from those of all other possible surface intermediates such as cyclohexane (C_6H_{12}), di-σ cyclohexene (C_6H_{10}), π-allyl C_6H_9, 1,3- and 1,4-cyclohexadienes (C_6H_8), and benzene (C_6H_6).[41]

The similarity and difference between the SFG spectra of π-allyl C_6H_9 and cyclohexyl are worth discussion. Both of the spectra are featured by symmetric and asymmetric CH_2 stretches. The difference in the relative band intensities between π-allyl c-C_6H_9 and cyclohexyl can be understood by considering the difference in their adsorption geometries on Pt(111). The relative SFG intensity of the CH_2 stretches is sensitive to the geometrical orientations of the CH_2 groups with respect to the surface normal.[11,12,42] For π-allyl c-C_6H_9, CH_2 groups at C_4, C_5, and C_6 positions can contribute to the SFG bands (see Scheme 1). Particularly, the transition dipole vector of the asymmetric stretch of the CH_2 group at C_5 position is nearly perpendicular to the metal surface, resulting in the strong SFG signal for the asymmetric CH_2 stretch at 2925 cm^{-1}. In contrast, the transition dipole vector of the symmetric stretch is nearly parallel to the metal surface, producing no SFG signal. Consequently, the SFG band at 2845 cm^{-1} is attributed to the symmetric C−H stretches at the C_4 and C_6 positions. The low-frequency tail in the band

at 2845 cm^{-1} is probably due to inhomogeneous interactions between the symmetric C−H stretches and the metal surface.

For cyclohexyl, the CH_2 group at C_4 makes a major contribution to the asymmetric SFG band at 2915 cm^{-1} (see Scheme 1). The transition dipole vectors of the asymmetric stretch at the C_2, C_3, C_5, and C_6 positions are nearly parallel to the surface, and thus only the CH_2 group at C_4 position can be SFG-active for the asymmetric stretching mode. For the CH_2 group at C_4, because the transition dipole vectors of the asymmetric and symmetric CH_2 stretches tilt approximately 36° and 54°, respectively, from the surface normal, the two stretches can produce comparably strong SFG signal. CH_2 groups at C_2, C_3, C_5, and C_6 positions tilt from the surface only by ∼18°, giving rise to a weak symmetric SFG band. Moreover, assuming negligible interactions with the metal surface, these four CH_2 groups constitute an inversion symmetry, which allows no SFG signal. In other words, the comparable SFG intensities of the two bands for cyclohexyl can be understood mainly by considering the orientation of the CH_2 group at C_4.

The decrease in the SFG intensity with increasing temperature is the result of the decrease in the surface coverage of cyclohexyl. At higher temperature, cyclohexyl can be more readily hydrogenated to form cyclohexane that eventually desorbs. In other words, increasing temperature increases the desorption rate of the cyclohexyl intermediate, via hydrogenation, resulting in a decrease of the SFG intensity. As an alternative possibility, the increase in the disordering of the cyclohexyl intermediate can cause a decrease in the SFG intensity because SFG is a coherent process. The relative intensity of the two bands at 2850 and 2915 cm^{-1} is slightly changed with temperature. This is due to the orientational changes of the surface species with temperature

It is interesting to compare the temperature dependence between cyclohexyl and π-allyl C_6H_9. As shown in Figure 2, as temperature increases, π-allyl C_6H_9 undergoes the irreversible dehydrogenation to form 1,3-cyclohexadiene and subsequently benzene. In contrast, the SFG spectrum for cyclohexyl changes reversibly with temperature. There is no indication of existing dehydrogenated species such as C_6H_{10}, C_6H_9, C_6H_8, and benzene during the heating/cooling cycle of cyclohexane. These observations strongly suggest that the dehydrogenation of cyclohexyl to form cyclohexene is a rate-limiting step in the cyclohexane catalytic conversion to benzene on Pt(111) in the presence of excess hydrogen. The dehydrogenation of cyclohexyl to cyclohexene competes with the backward reaction: hydrogenation of cyclohexyl, followed by desorption in a form of cyclohexane. According to the calculations by Koel et al.,[30] the activation energy (12 kcal/mol) of cyclohexyl dehydrogenation to adsorbed cyclohexene is lower than the activation energy (17 kcal/mol) of cyclohexyl hydrogenation to adsorbed cyclohexane. The presence of excess hydrogen, however, can inhibit the dehydrogenation and enhance the hydrogenation process.

Hydrogen Effect on Surface Species under 1.5 Torr of Cyclohexane at 310 K. The influence of excess hydrogen on the cyclohexane reaction pathway is highlighted in Figure 8. In Figure 8, the SFG spectrum at 310 K under 1.5 Torr of cyclohexane in the absence of excess hydrogen (Figure 8a) is compared with that in the presence of excess hydrogen (Figure 8b). The weak band at 3000 cm^{-1} in Figure 8a is assigned to the aromatic C−H stretch from adsorbed benzene and/or phenyl.[14] The two bands at 2845 and 2925 cm^{-1} are consistent with characteristics of π-allyl c-C_6H_9. The SFG spectrum in Figure 8b corresponds to cyclohexyl. Note that, in the presence of excess hydrogen, the dehydrogenation of cyclohexyl to π-allyl

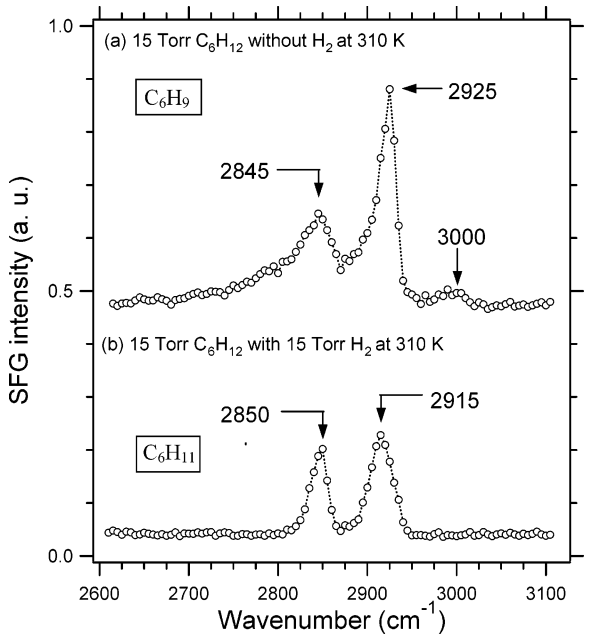

Figure 8. SFG spectra of surface species on Pt(111) at 310 K under 1.5 Torr of cyclohexane (a) in the absence and (b) in the presence of 15 Torr of H_2.

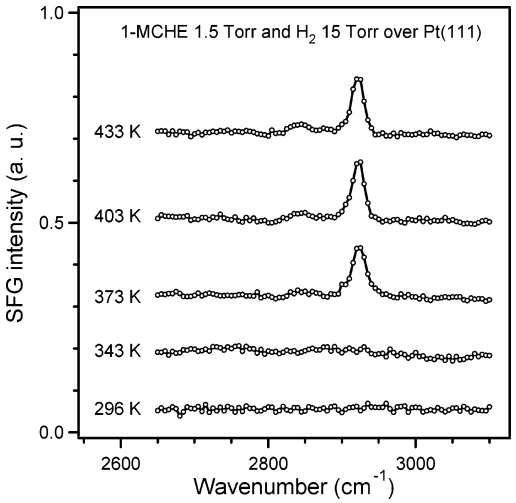

Figure 9. Temperature-dependent SFG spectra of surface species on Pt(111) under 1.5 Torr of 1-methylcyclohexene (1-MCHE) and 15 Torr of H_2.

C_6H_9 was not accessible even after the sample had been heated to 453 K. The dehydrogenation becomes facile even at 310 K in the absence of hydrogen.

3.3. Adsorption Structure and Reactions of 1-Methylcyclohexene on Pt(111). *Temperature Dependence of Surface Species and Reaction Rates under 1.5 Torr of 1-Methylcyclohexene and 15 Torr of H_2.* The temperature-dependent SFG spectra of the surface species on Pt(111) under 1.5 Torr of 1-methylcyclohexene and 15 Torr of H_2 are shown in Figure 9. No SFG peak in the C−H stretching region appeared until 373 K, at which point two major bands were shown at 2845 and 2925 cm^{-1}. The intensity of the two bands remained the same upon heating to 433 K.

The bands at 2845 and 2925 cm^{-1} are typical symmetric and asymmetric C−H stretches, respectively, of a CH_2 group. Note that the SFG spectrum in Figure 9 is almost the same as that of π-allyl *c*-C_6H_9 in terms of the positions and relative intensities of the two bands. We suggest methylcyclohexenyl as the surface species responsible for the SFG spectra. Scheme 1e illustrates

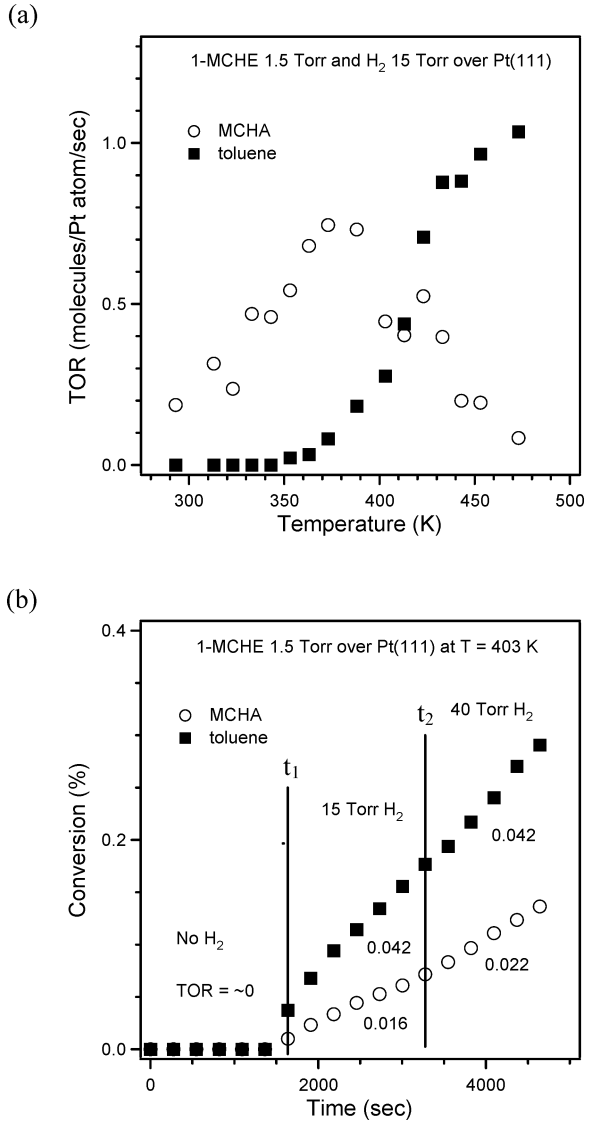

Figure 10. (a) Turnover rates (TORs) of the hydrogenation to methylcyclohexane (MCHA) and the dehydrogenation to toluene of 1-methylcyclohexene (1-MCHE) at 1.5 Torr in the presence of 15 Torr of H_2 as a function of temperature and (b) the fractional change of methylcyclohexane and toluene in the gas composition as a function of time. In b, the H_2 pressure was kept at zero at $0 < t < t_1$, 15 Torr at $t_1 < t < t_2$, and 40 Torr at $t > t_2$.

one possible molecular structure of methylcyclohexenyl species, π-allyl c-C_6H_8−$CH_{2,a}$. The methylcyclohexenyl intermediate lacks a CH_3 group by forming a σ-bond to the surface. Another possible molecular structure of methylcyclohexenyl is the one with the CH_3 group remaining intact on the surface (π-allyl c-C_6H_8−$CH_{3,a}$). This surface species has been observed upon methylcyclohexane adsorption on Pt(111).[43]

Kinetic measurements for the 1-methylcyclohexene catalytic reactions on Pt(111) were performed under 1.5 Torr of 1-methylcyclohexene and 15 Torr of H_2. The TORs for hydrogenation to methylcyclohexane and dehydrogenation to toluene are shown in Figure 10a as a function of temperature. We emphasize that the onset (about 360 K) of the appearance of the peaks in the SFG spectrum matches the onset of the production of toluene in the GC results. This indicates that methylcyclohexenyl is a reactive surface intermediate in the process of 1-methylcyclohexene dehydrogenation to toluene.

Hydrogen Effect on Surface Species and Reaction Rates under 1.5 Torr of 1-Methylcyclohexene at 403 K. An unusual hydrogen effect on the dehydrogenation rate is shown in Figure 10b. The time evolution of the gas composition during a GC measurement was recorded initially under 1.5 Torr of 1-methylcyclohexene at 403 K in the absence of excess hydrogen, and subsequently, H_2 was added. Figure 10b shows the change in the gas composition of methylcyclohexane and toluene as a function of time. The catalytic conversions were negligible in a period of $0 < t < t_1$, in which there is no excess hydrogen. When 15 Torr of H_2 was added at $t = t_1$, surprisingly, the dehydrogenation and hydrogenation reactions began with constant rates (TOR = 0.042 and 0.016, respectively). The TORs remained the same after a total of 40 Torr of H_2 was added at $t = t_2$.

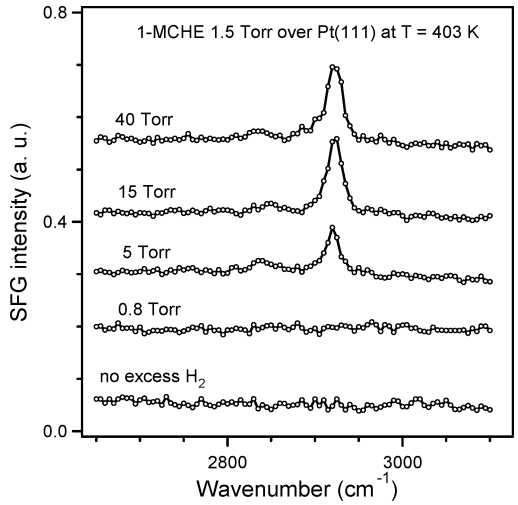

Figure 11. SFG spectra of surface species on Pt(111) at 403 K under 1.5 Torr of 1-methylcyclohexene with varying H_2 pressure.

The SFG results in Figure 11 show how excess hydrogen affects the adsorption of the reactant during the catalytic reactions. The SFG spectra were taken while the pressure of H_2 in the reaction cell was increased in a stepwise manner from 0 to 40 Torr in 1.5 Torr of 1-methylcyclohexene. No SFG bands were observed until 5 Torr of H_2 had been added. The SFG bands increased slightly at 15 Torr of H_2 and their intensity remained the same at 40 Torr of H_2. This result indicates that excess hydrogen on the surface plays a critical role in initiating the formation of the surface intermediate on Pt(111). Another experiment found that, in the absence of excess hydrogen, no SFG band was detected in the temperature range 293−453 K and under 1.5 Torr of 1-methylcyclohexene. This indicates that the chemisorption of 1-methylcylochexene is a slow step, which is likely because steric hindrance by the methyl group prohibits 1-methylcyclohexene from forming a di-σ-bonded adsorbate on Pt(111).

On the basis of the GC and SFG results, we suggest that excess hydrogen on the surface can activate a different reaction pathway for the formation of methylcyclohexenyl. The chemisorption of 1-methylcyclohexene can be accessed by hydrogenation to methylcyclohexyl, C_7H_{13}(a), in the presence of excess hydrogen (reaction R1 below). Öfner et al.[44] have reported that ethyl (C_2H_5) formation from weakly π-bonded ethylene (C_2H_4) on a hydrogen-precovered Pt(111) is facile, and the complete hydrogenation of ethylene to ethane requires an activation energy of only 6 kcal/mol. A methylcyclohexyl intermediate then undergoes a disproportionation reaction with a weakly π-bonded 1-methylcyclohexene in excess to form a methylcyclohexane, C_7H_{14}(g) and a dehydrogenated species, C_7H_{11}(a) (reaction R2). The C_7H_{11} intermediate is dehydrogenated to C_7H_{10}(a), followed by further dehydrogenation to form adsorbed

toluene that eventually desorbs into the gas phase [C_7H_8(g), reaction R3]

$$C_7H_{12}(\pi) + H(a) \rightarrow C_7H_{13}(\sigma) \quad (R1)$$

$$C_7H_{13}(\sigma) + C_7H_{12}(\pi) \rightarrow C_7H_{14}(g) + C_7H_{11}(a) \quad (R2)$$

$$C_7H_{11}(a) \rightarrow C_7H_{10}(a) + H(a) \rightarrow C_7H_8(g) + 3H(a) \quad (R3)$$

where π, σ, and a represent weakly π-bonded, σ-bonded, and strongly chemisorbed molecules, respectively, and g represents product molecule in the gas phase. This reaction mechanism predicts the production of both methylcyclohexane and toluene by excess hydrogen, which is consistent with the GC result shown in Figure 10, where the post-introduction of hydrogen initiated the productions of both methylcyclohexane and toluene.

3.4. Adsorption Structures of C_6 Linear Hydrocarbons at 296 K: Hexane, 3-Methylpentane, 2-Methylpentane, and 1-Hexene. C_6 linear hydrocarbons on Pt(111) are more complicated systems than C_6 cyclic hydrocarbons on Pt(111) in that more conformers and reaction pathways exist because of rotational degrees of freedom by C−C bond rotation. In addition, C_6 linear hydrocarbons contain vibrational modes of both CH_2 and CH_3, whereas C_6 cyclic hydrocarbons contain mainly CH_2 vibrational modes, as described above. Therefore, in the cases of C_6 linear hydrocarbons, it is necessary to set the criteria for the assignment of SFG bands and the identification of corresponding chemical species on the surface. First, when C_6 alkanes are physisorbed on Pt(111), they align on the surface such that the number of carbon chains bonding to the metal surface is maximized. This has proven to be the case for *n*-alkanes (C_NH_{2N+2}, $N > 4$) on Au and Pt surfaces.[45−47] Adsorption energy of the *n*-alkanes increases with increasing number of carbon chains: for example, the binding energy per carbon chain for *n*-alkanes ($6 < N < 10$) on Pt(111) is about 2.1 kcal/mol.[45] Second, when C_6 alkanes and C_6 alkenes are dehydrogenated, they exist on the surface in largely two adsorption geometries: "flat-lying" and "standing-up" as in the case of hexylidyne in Scheme 1. The standing-up geometry can be more favorable than the flat-lying geometry when van der Waals interactions between adjacent carbon chains are dominant over carbon chain−metal interactions. This is well-known for various self-assembled monolayer systems of long-chain hydrocarbons on metal surfaces such as Au, Ag, and Pt.

The reference IR band positions for the CH stretching modes of interest are summarized in Figure 12. The IR spectrum for a standing-up adsorbate features symmetric stretches of CH_3 and CH_2 groups. These symmetric stretches are denoted as CH_3(s) and CH_2(s), for further discussion. These bands appear at about 2875 and 2850 cm^{-1}, respectively, similar to those in the condensed phase. The IR spectrum for a flat-lying adsorbate on Pt(111) features asymmetric stretches of CH_2 and CH_3 groups. These bands are red-shifted by 20−40 cm^{-1} from those in the condensed phase because of their interactions with the metal surface. As a result, asymmetric CH_3 and CH_2 stretches, perturbed by the surface, appear at about 2920 and 2900 cm^{-1}, respectively. These two bands are denoted as CH_3(a,p) and CH_2(a,p), respectively. Finally, unperturbed symmetric stretches of CH_3 and CH_2, denoted as CH_3(s) and CH_2(s), appear at about 2960 and 2920 cm^{-1}, respectively.

The SFG spectra of surface species on Pt(111) at 296 K under 1.5 Torr of C_6 linear hydrocarbons and 15 Torr of H_2 are shown in Figure 13. In order from the top in Figure 13 are *n*-hexane, 3-methylpentane, 2-methylpentane, and 1-hexene. To simplify the fitting of the SFG spectra, all resonance terms in eq 4 were

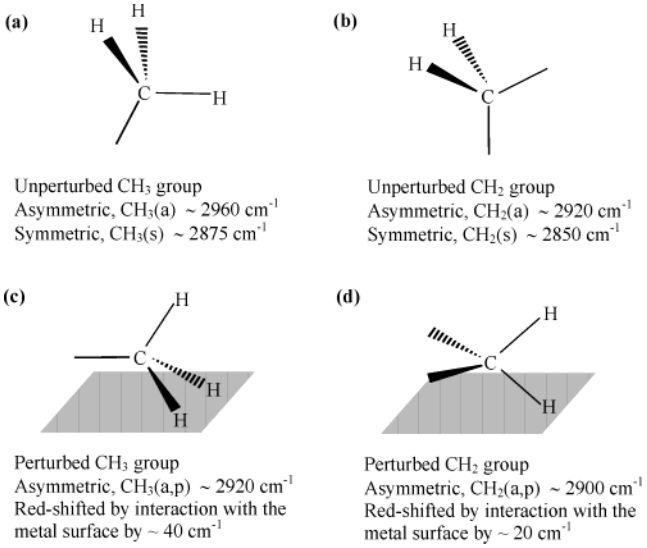

Figure 12. Schematic diagram of CH stretching modes.

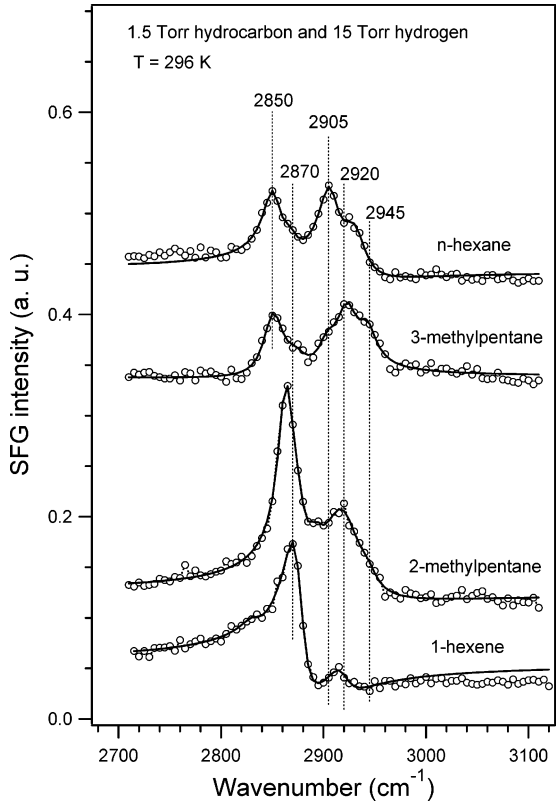

Figure 13. SFG spectra of surface species on Pt(111) at 296 K under 1.5 Torr of C_6 hydrocarbons and 15 Torr of H_2. In order from the top are *n*-hexane, 3-methylpentane, 2-methylpentane, and 1-hexene. The solid lines correspond to fits using eq 5.

assumed to be in phase; that is, the phase factor ϕ_q is independent of the vibrational mode. This assumption was previously used to analyze SFG spectra from *n*-alkanethiol monolayers on gold surfaces.[10] Then, eq 4 can be rewritten as

$$I_{SF} \propto \left| |\chi_{NR}| e^{i\theta} + \sum_q \frac{|A_q|}{\omega_{IR} - \omega_q + i\Gamma_q} \right|^2 I_{VIS} I_{IR} \quad (5)$$

where θ is the phase difference between the nonresonance and resonance components. The solid lines in Figure 13 correspond to fits using eq 5 with the fitting parameters $|\chi_{NR}|$, θ, $|A_q|$, ω_q,

TABLE 1: Fitting Results to Eq 5 and Assignments for the SFG Spectra of *n*-Hexane, 3-Methylpentane, 2-Methylpentane, and 1-Hexene at 296 K on Pt(111) at High Pressure (1.5 Torr) with 15 Torr of H_2

mode		*n*-hexane	3-methylpentane	2-methylpentane	1-hexene
CH_2(s)	ω_q	2851 ± 0.8	2850 ± 0.9		2833 ± 2.8
	$\|A_q\|$	0.40 ± 0.07	0.47 ± 0.06		0.077 ± 0.03
	Γ_q	10.3 ± 1.2	11.5 ± 1.5		10.8 ± 5.4
CH_3(s)	ω_q	2868 ± 0.1	2872 ± 4.7	2865 ± 2.5	2870 ± 0.4
	$\|A_q\|$	0.13 ± 0.07	0.07 ± 0.03	1.18 ± 0.96	1.06 ± 0.03
	Γ_q	10.0 ± 4.0	10.2 ± 2.3	9.1 ± 2.9	11.3 ± 0.42
CH_2(a,p)	ω_q	2907 ± 0.5	2903 ± 3.6	2893 ± 2.6	
	$\|A_q\|$	0.54 ± 0.07	0.15 ± 0.17	0.10 ± 0.10	
	Γ_q	11.8 ± 1.1	9.9 ± 6.5	7.9 ± 6.1	
CH_3(a,p)	ω_q	2931 ± 1.0	2922 ± 1.7		
	$\|A_q\|$	0.44 ± 0.08	0.51 ± 0.12		
	Γ_q	14.0 ± 1.8	13.0 ± 5.7		
CH_3(FR)	ω_q			2920 ± 2.0[a]	2917 ± 1.4
	$\|A_q\|$			1.28 ± 0.25	0.22 ± 0.06
	Γ_q			22.5 ± 3.1	13.0 ± 3.4
CH_3(a)	ω_q		2942 ± 2.3	2944 ± 4.1	
	$\|A_q\|$		0.19 ± 0.15	0.08 ± 0.09	
	Γ_q		9.5 ± 4.5	10.0 ± 9.7	

[a] This SFG band includes a contribution from the symmetric stretch of a CH_2 group on carbons bonded to the surface (α- and γ-positions). See text for details.

SCHEME 2

(a) At low pressure (<10^{-6} Torr, in UHV environments)

Cyclohexene (C_6H_{10}) $\xrightarrow[\text{Pt(111)}]{100\text{ K}}$ di-σ cyclohexene (C_6H_{10}) $\xrightarrow{200\text{ K}}$ π-allyl c-C_6H_9 $\xrightarrow{300\text{ K}}$ Benzene (C_6H_6)

(b) At high pressure (with and without 15 Torr H_2)

Cyclohexene (1.5 Torr) (C_6H_{10}) $\xrightarrow[\text{Pt(111)}]{\sim 303\text{ K}}$ 1,4-cyclohexadiene (C_6H_8) $\xrightarrow{\sim 323\text{ K}}$ π-allyl c-C_6H_9 $\xrightarrow{\sim 423\text{ K}}$ Benzene (C_6H_6)

Cyclohexene (1.5 Torr) + H_2 (15 Torr) $\xrightarrow[\text{Pt(111)}]{\sim 303\text{ K}}$ 1,4-cyclohexadiene, 1,3-cyclohexadiene (C_6H_8) $\xrightarrow{\sim 323\text{ K}}$ π-allyl c-C_6H_9 $\xrightarrow{\sim 400\text{ K}}$ 1,3-cyclohexadiene (C_6H_8)

and Γ_q. The parameters $|A_q|$, ω_q, and Γ_q determined from the fits are summarized in Table 1.

The limitation arises from the facts that the fitting was performed under the assumption of identical ϕ_q's and $|A_q|$ contains the Fresnel factors that depend on the vibrational modes. Despite the fact that the Fresnel factors were not separable in our analysis, we believe that the relative magnitudes of $|A_q|$ between the vibrational modes still reflect the molecular orientations, as discussed in section 2.2. As shown in Figure 13 and Table 1, the relative magnitudes of $|A_q|$ between the vibrational modes vary (dramatically in some cases) with different molecules. This is due to different molecular orientations from corresponding surface species rather than different Fresnel factors that are similar for those C_6 hydrocarbons.

For the SFG spectrum of *n*-hexane, there are three major bands at 2851, 2907, and 2931 cm^{-1} with a weak band at 2868 cm^{-1} (Table 1). The three major bands are assigned to unperturbed symmetric CH_2 [CH_2(s)], perturbed asymmetric CH_2 [CH_2(a,p)], and perturbed asymmetric CH_3 [CH_3(a,p)] stretching modes, respectively. The weak band at 2868 cm^{-1} is assigned to unperturbed symmetric CH_3 [CH_3(s)] stretching mode. The strong CH_3(a,p) peak indicates that the CH_3 groups align with their 3-fold rotational symmetry axis parallel to the surface, interacting with the metal surface. In addition, the strong CH_2(a,p) peak indicates that the 2-fold rotational symmetry axis of the CH_2 groups is also parallel to the surface, interacting with the surface. These features are consistent with characteristics of the flat-lying *n*-hexane in the TTT conformation.[47−49] The band at 2851 cm^{-1}, assigned to CH_2(s), is not SFG active for the flat-lying *n*-hexane in the TTT conformation. Observation of this band in the SFG spectrum implies that different conformers of *n*-hexane exist on the surface at 296 K. Molecular dynamics (MD) calculations[50] suggest that *n*-hexane on Pt(111) exists in the TTT conformation below 200 K but that, above 200 K, torsional motions around C−C bonds are thermally activated, giving rise to an increase in the fraction of conformational isomers in the gauche states. Proposed adsorption geometry of *n*-hexane at 296 K is illustrated in Scheme 2a.

The SFG spectrum for 3-methylpentane is similar to that for *n*-hexane. The two major bands at 2850 and 2922 cm^{-1} are assigned to CH_2(s) and CH_3(a,p), respectively. The three weak bands at 2872, 2903, and 2942 cm^{-1} are assigned to CH_3(s), CH_2(a,p), and CH_3(a), respectively. The strong CH_3(a,p) peak compared with the CH_3(s) peak indicates that CH_3 groups mainly align with their 3-fold rotational symmetry axis parallel to the surface, interacting with the metal surface. One difference from *n*-hexane is that the band at 2903 cm^{-1}, corresponding to CH_2(a,p), is weaker than that for *n*-hexane. Another difference is the appearance of a new band at 2942 cm^{-1}, which is assigned to CH_3(a). The proposed adsorption geometry of 3-methylpentane at 296 K is illustrated in Scheme 2b, where two CH_2 groups and two terminal CH_3 groups are in contact with the metal surface while a central CH_3 group tilts away from the surface. This adsorption geometry can explain qualitatively our observations that $|A_q[CH_3(a,p)]|$ for 3-methylpentane is similar to that for *n*-hexane, whereas $|A_q[CH_2(a,p)]|$ for 3-methylpentane is

SCHEME 3

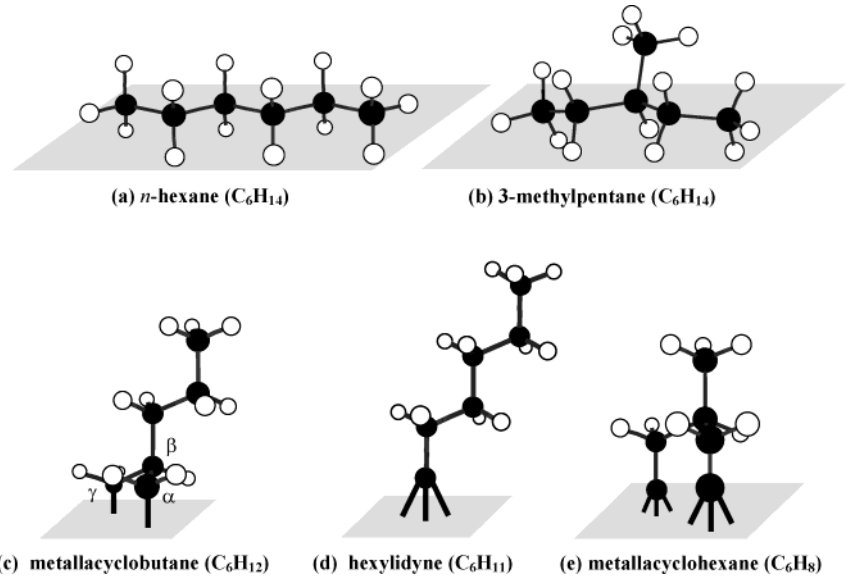

smaller than that for *n*-hexane. This is because $|A_q|$ scales with the number of the CH groups responsible for the q_{th} mode in an adsorbate.

The SFG spectrum for 2-methylpentane is different from those for *n*-hexane and 3-methylpentane. The strong band at 2865 cm^{-1} is assigned to the unperturbed symmetric CH_3 stretch [CH_3(s)]. The predominant CH_3(s) peak over the CH_3(a) and CH_2(a,p) peaks indicates that the 3-fold rotational symmetry axis for the CH_3 groups is nearly perpendicular to the metal surface. In addition, the very weak CH_2(a,p) peak indicates that the CH_2 groups are not in contact with the metal surface, as opposed to *n*-hexane and 3-methylpentane. These features represent the characteristics of standing-up geometry where the molecular plane is perpendicular to the metal surface. We propose that 2-methylpentane exists as a metallacyclobutane on Pt(111) at 296 K, in which two carbon atoms in α- and γ-positions bind with the surface through σ-bonding, as illustrated in Scheme 2c. The formation of metallacyclic species on Pt(111) through γ-hydride elimination has been reported from thermal decomposition of adsorbed neopentyl species [$(CH_3)_3$-CH_2−] at 235 K.[51] The peak centered at 2920 cm^{-1} has a much broader line width ($\Gamma_q = 23$ cm^{-1}) than other bands, implying that it consists of more than one CH stretching mode. One possible contribution is the symmetric stretch of a CH_2 group on carbons bonded to the surface (α- and γ-positions). This stretching mode has been observed in the RAIRS and SFG spectra of σ-bonded hydrocarbons (C_2−C_6) on Pt(111) at 2900−2920 cm^{-1}.[31,52,53] Another possible contribution is the Fermi resonance [CH_3(FR)] of the CH_3 stretching mode by interaction with an overtone of a CH_3 bending mode.[10,54,55]

Similarly to the case of 2-methylpentane, the SFG spectrum for 1-hexene features a strong band at 2870 cm^{-1}, which is assigned to CH_3(s). We propose that major surface species responsible for the SFG spectrum is a hexylidyne (C_6H_{11}) intermediate, as illustrated in Scheme 2d. The two weak bands at 2833 and 2917 cm^{-1} are most likely CH_2(s) and CH_3(FR), respectively. Hexylidyne was previously observed upon 1-hexene adsorption on Pt(111) under UHV conditions.[52] The absence of the CH_3(a) band in our SFG spectrum indicates that the TTT conformer is dominant over the GTT conformer. The reason is probably that 1-hexene adsorption on Pt(111) at high pressure (1.5 Torr) results in the formation of a self-assembled monolayer of densely packed hexylidyne on the surface in the TTT conformation, due to substantial intermolecular interactions.

3.5. Surface Chemistry of the Linear C_6 Hydrocarbons at Various Temperatures in the Presence and Absence of Excess Hydrogen. *Influences of Temperature and Excess Hydrogen on Surface Species under 1.5 Torr of the Linear C_6 Hydrocarbons.* The temperature-dependent SFG spectra of surface species on Pt(111) under 1.5 Torr of *n*-hexane and 15 Torr of hydrogen are shown in Figure 14. The sample was initially kept at 296 K and then heated sequentially for each SFG measurement. After being heated to 453 K, the sample was cooled to 310 K to examine the surface chemistry during a heating/cooling cycle.

The SFG spectrum for *n*-hexane at 296 K features the three major bands at 2851 [CH_2(s)], 2907 [CH_2(a,p)], and 2931 cm^{-1} [CH_3(a,p)], as described in the previous section. The appearance of these bands along with negligible bands for CH_3(s) and CH_3(a) is indicative of the flat-lying adsorption geometry. Upon heating of the surface, the bands broaden and their intensities decrease, becoming featureless at 453 K. A new band above 3000 cm^{-1} at 373 K arises, probably from vinyl or aromatic CH stretch.[14,52] After the heating/cooling treatment, two new bands appear: a strong band at 2870 cm^{-1} [CH_3(s)] and a weak band at 2950 cm^{-1} (CH_3(a)).

The appearance of the new bands, CH_3(s) and CH_3(a), after the heating/cooling treatment indicates that a new surface species was formed through an irreversible pathway, that is, a dehydrogenation process. Because the CH_3(s) peak is much stronger than the CH_3(a) peak, the new species is likely in a standing-up geometry. One possible species is hexylidyne in the TTT conformation (Scheme 1d). Its conformers such as GTT might coexist, making contribution to CH_3(a) (2950 cm^{-1}).[52] Alkylidyne on Pt(111) is formed by subsequent α-hydride elimination from adsorbed alkyl or alkene groups. Studies at low pressures revealed that alkylidyne formation on Pt(111) occurs at 200−300 K for C_2−C_6 alkyl and alkene molecules.[31,51,52,56] Another possible species in a standing-up geometry is metallacyclobutane or metallacyclohexane. These metallacyclic species are believed to be surface intermediates when *n*-hexane is isomerized to 2- or 3-methylpentane and vice versa.[2]

Similar temperature dependence for SFG spectra was observed in the case of 3-methylpentane. Upon heating of the

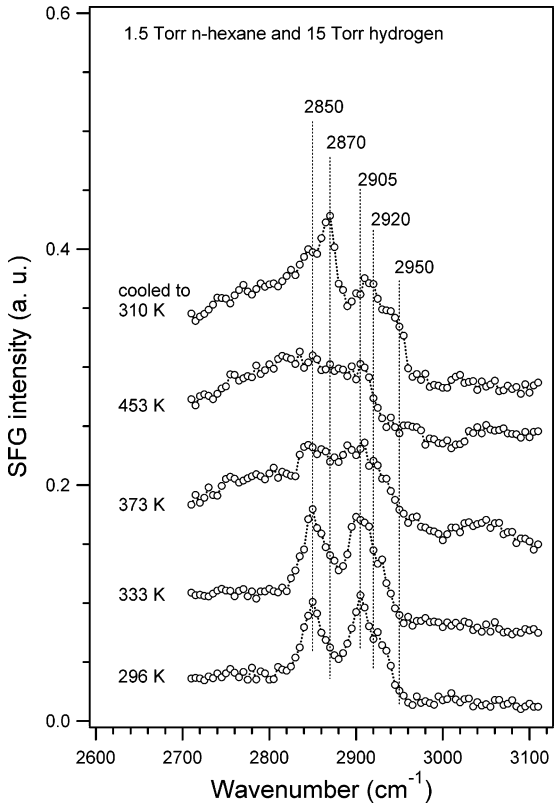

Figure 14. Temperature-dependent SFG spectra of surface species on Pt(111) under 1.5 Torr of *n*-hexane and 15 Torr of H_2 in the temperature range of 296−453 K. The metal surface was initially kept at 296 K and then heated sequentially for each SFG measurement. The SFG spectrum on the top was obtained after the surface was cooled to 310 K.

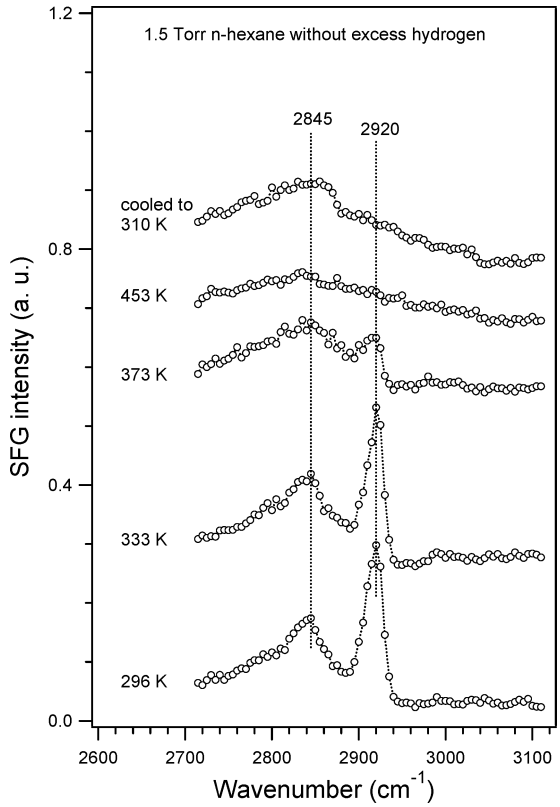

Figure 15. Temperature-dependent SFG spectra of surface species on Pt(111) under 1.5 Torr of *n*-hexane in the absence of excess hydrogen in the range 296−453 K. The SFG spectrum on the top was obtained after the surface was cooled to 310 K.

sample, the SFG bands broaden and their intensities decrease. After the heating/cooling treatment, a strong band appears at 2870 cm^{-1}, assigned to CH_3(s). A proposed surface intermediate responsible for the new band is a metallacyclohexane (Scheme 2e). Contrary to the cases of *n*-hexane and 3-methylpentane, it was found that the heating/cooling treatment induced little change in the SFG spectra for 2-methylpentane and 1-hexene. These results indicate that metallacyclic species and hexylidyne are thermally stable species on Pt(111) in the temperature range 296−453 K. This is consistent with our findings that adsorbed *n*-hexane and 3-methylpentane converted into metallacyclic species or hexylidyne upon heating to 453 K.

The temperature-dependent SFG spectra in 1.5 Torr of *n*-hexane in the absence of excess hydrogen are shown in Figure 15. The surface chemistry of *n*-hexane in the absence of excess hydrogen is astonishingly different from that in the presence of excess hydrogen. The SFG spectrum at 296 K in Figure 15 features two bands at 2845 and 2920 cm^{-1}. The characteristics of the two SFG bands, in terms of peak positions and relative breadths and intensities, match well those of a cyclohexenyl, π-allyl c-C_6H_9 intermediate. One might attempt to assign the band at 2920 cm^{-1} to the CH_3(a,p) mode rather than the CH_2(a) mode. However, it was impossible to find any reasonable adsorption geometry that can be characterized by the CH_2(s) and CH_3(a,p) bands. Similarly to the case of the presence of excess hydrogen, the SFG bands decreased and became featureless with increasing temperature. The main difference is that, for *n*-hexane, the two SFG band (2845 and 2920 cm^{-1}) at 296 K, assigned to π-allyl c-C_6H_9, disappeared after the heating/cooling treatment. This is due to irreversible dehydrogenation of the intermediate to form benzene or phenyl groups.[23]

For 2-methylpentane, 3-methylpentane, and 1-hexene, they were found to be mostly in standing-up geometries, such as hexylidyne and metallacyclic species. They remained unreacted after the heating/cooling treatment.

Elucidating the Reaction Mechanisms of Isomerization and Dehydrocyclization of n-Hexane. One of the most interesting observations in the study of the linear C_6 hydrocarbons is the formation of π-allyl c-C_6H_9 from *n*-hexane at 296 K in the absence of excess hydrogen. In the presence of excess hydrogen, *n*-hexane adsorbs molecularly on Pt(111) at 296 K. Upon heating, it converts into different surface species with standing-up geometry, most likely either hexylidyne via stepwise α-hydride elimination or metallacyclic species via hydrogenolysis of methylcyclopentane. Without excess hydrogen, dehydrocyclization of *n*-hexane to π-allyl c-C_6H_9 occurs predominantly even at 296 K. Neither metallacyclic species nor hexylidyne were detected during the heating/cooling cycle of π-allyl c-C_6H_9 in the range 290−450 K and vice versa. This implies that dehydrocyclization of *n*-hexane to form π-allyl c-C_6H_9 proceeds via different reaction pathway from dehydrogenation of *n*-hexane to form hexylidyne or metallacyclic species. Our SFG studies of high-pressure cyclohexene (C_6H_{10}) on Pt(111) showed that π-allyl c-C_6H_9 is a reactive intermediate in the cyclohexene conversion to benzene: π-allyl c-C_6H_9 converts into 1,3-cyclohexadiene (C_6H_8) and is followed by benzene formation. All of these results lead us to conclude that π-allyl c-C_6H_9 is a reactive surface intermediate for dehydrocylization of *n*-hexane to benzene. This conclusion supports the proposed mechanism of direct 1,6-ring closure[4] rather than ring enlargement of methylcyclopentane for dehydrocylization of *n*-hexane. Furthermore, we propose that direct 1,6-ring closure takes place via the formation of cyclohexane followed by consecutive

dehydrogenation rather than the consecutive dehydrogenation of *n*-hexane to hexene−hexadiene−hexatriene followed by cyclization.

Isomerization of *n*-hexane on Pt(111) to form 2- or 3-methylpentane at high pressures and temperatures is believed to occur via formation of a methylcyclopentane intermediate followed by its hydrogenolysis.[2,4,57] It has been speculated that this reaction pathway should include metallacyclic species as a reactive intermediate.[2,58] Our SFG results showed that metallacyclic species and hexylidyne from the C_6 hydrocarbons were formed either by heating to 450 K in the presence of excess hydrogen or at room temperature in the absence of excess hydrogen. This leads us to suggest that metallacyclic species and hexylidyne are reactive intermediates in the process of *n*-hexane isomerization through methylcyclopentane formation. Note that this reaction pathway is distinctive from dehydrocylization of *n*-hexane to benzene.

Finally, we discuss the effect of hydrogen on the reaction pathways in the *n*-hexane reforming process. Davis et al.[4] reported from GC measurements during the *n*-hexane reforming reactions on Pt(111) that the gas product ratio of benzene to methylcyclopentane increases with decreasing hydrogen pressure; that is, dehydrocylization of *n*-hexane to benzene is favored over cyclization to methylcyclopentane in hydrogen-deficient environments. Our spectroscopic measurements of the surface species during the reactions show that dehydrocylization of *n*-hexane is the dominant pathway in the absence of excess hydrogen over isomerization of *n*-hexane. This is consistent with the GC results by Davis et al.[4]

4. Summary

Using the SFG surface vibrational technique, we have identified surface species on Pt(111) under high pressures of C_6 linear and cyclic hydrocarbons in the presence and absence of excess hydrogen and as a function of temperature. Upon cyclohexene adsorption on Pt(111), 1,3- and 1,4-cyclohexadienes and π-allyl C_6H_9 were observed. Of these species, 1,3- and 1,4-cyclohexadienes have never been observed in the case of cyclohexene adsorption at low pressures. Upon cyclohexane adsorption, cyclohexyl and π-allyl C_6H_9 were formed on the surface in the presence and absence of excess hydrogen, respectively. Adsorption of 1-methylcyclohexene resulted in the formation of methylcyclohexenyl in the presence of excess hydrogen. The presence of excess hydrogen assisted the chemisorption that was otherwise inhibited by steric hindrance in the absence of hydrogen.

n-Hexane and 3-methylpentane adsorbed molecularly on Pt(111) at 296 K in the presence of excess hydrogen. 2-Methylpentane and 1-hexene were readily dehydrogenated to form metallacyclobutane and hexylidyne even at 296 K, regardless of the presence of excess hydrogen. *n*-Hexane was dehydrogenated to form hexylidyne or metallacyclic species at high temperature in the presence of excess hydrogen. Hexylidyne and metallacyclic species were also main surface intermediates in dehydrogenation of 2- and 3-methylpentane. The absence of excess-hydrogen-induced dehydrocyclization of *n*-hexane to form π-allyl c-C_6H_9. The SFG results support the conclusion that the benzene formation from *n*-hexane on Pt(111) does not proceed via a five-member cyclic intermediate as does isomerization, but rather proceeds through a direct 1,6-ring closure.

The SFG surface vibrational technique allowed us to study the influence of excess hydrogen on surface species. Excess hydrogen on the surface caused the broadening and intensity decrease of the SFG bands corresponding to π-allyl C_6H_9. This can be explained by an increase in the disordering and decrease in the surface coverage of the C_6H_9 due to the weakening of the hydrocarbon−Pt bond. In some cases, excess hydrogen participated as a reactant in dehydrogenation. Excess hydrogen prevented dehydrogenation for cyclohexyl but enhanced dehydrogenation for 1-methylcyclohexene.

The SFG technique combined with kinetic measurements provided a unique capability of investigating reactive intermediates and elementary steps by probing surface species and monitoring gas products simultaneously. In the case of cyclohexene adsorption on Pt(111), the onset temperature of 1,3-cyclohexadiene formation on the surface was consistent with that of the benzene production in the gas phase. This indicates that 1,3-cyclohexadiene is a reactive intermediate in cyclohexene dehydrogenation to benzene. For the same reason, methylcyclohexenyl was found to be a reactive intermediate in 1-methylcyclohexene dehydrogenation to toluene. Another example is found in the case of the SFG and GC results for the cyclohexene reaction in the absence of excess hydrogen. The SFG results showed that, in the absence of excess hydrogen, the cyclohexene reaction on Pt(111) is dictated by bimolecular reactions between surface species and cyclohexene reactant. This is correlated with the results from the kinetic measurements that both cyclohexane and benzene are produced via disproportionation rather than stepwise hydrogenation/dehydrogenation.

It is likely that other platinum crystal surfaces might also stabilize other reaction intermediates in the route of *n*-hexane conversion to branched isomers or benzene. The platinum (111) surface is the least reactive of all platinum surfaces in activating C−H bonds, and therefore, most of the interesting intermediates can be kept relatively intact when adsorbed on this crystal face. It is our hope that the more active stepped and atomically rougher surfaces can also participate in chemistry of the C_6 species in ways that correlate well with our studies using the Pt(111) crystal face.

Acknowledgment. This work was supported by the Director, Office of Energy Research, Office of Basic Energy Sciences, and Materials Science Division, of the U.S. Department of Energy under Contract No. DE-AC03-76SF00098.

References and Notes

(1) *Catalytic Naphtha Reforming: Science and Technology*; Antos, G. J.; Aitani, A. M.; Parera, J. M., Eds.; Marcel Dekker: New York, 1995.
(2) Davis, B. H. *Catal. Today* **1999**, *53*, 443.
(3) *Hydrogen Effects in Catalysis: Fundamentals and Practical Applications*; Paál, Z., Mennon, P. G., Eds.; Marcel Dekker: New York, 1988.
(4) Davis, S. M.; Zaera, F.; Somorjai, G. A. *J. Catal.* **1984**, *85*, 206.
(5) Paál, Z. *Adv. Catal.* **1980**, *29*, 273.
(6) Dumestic, J. A.; Milligan, B. A.; Greppi, L. A.; Balse, V. R.; Sarnowski, K. T.; Beall, C. E.; Kataoka, T.; Rudd, D. F.; Trevino, A. A. *Ind. Eng. Chem. Res.* **1987**, *26*, 1399.
(7) Shen, Y. R. *Nature* **1989**, *337*, 519.
(8) Shen, Y. R. *The Principles of Nonlinear Optics*; Wiley: New York, 1984.
(9) Shen, Y. R. *Annu. Rev. Phys. Chem.* **1989**, *40*, 327.
(10) Himmelhaus, M.; Eisert, F.; Buck, M.; Grunze, M. *J. Phys. Chem. B* **2000**, *104*, 576.
(11) Hirose, C.; Akamatsu, N.; Domen, K. *J. Chem. Phys.* **1992**, *96*, 997.
(12) Wei, X.; Hong, S.; Zhuang, X.; Goto, T.; Shen, Y. R. *Phys. Rev. E* **2000**, *62*, 5160.
(13) Sheppard, N. *Annu. Rev. Phys. Chem.* **1988**, *39*, 589.
(14) Sheppard, N.; Cruz, C. D. L. *Adv. Catal.* **1998**, *42*, 181.
(15) Nichols, H.; Hexter, R. M. *J. Chem. Phys.* **1980**, *73*, 965.
(16) Hallmark, V. M.; Campion, A. *J. Chem. Phys.* **1986**, *84*, 2942.
(17) Kung, K. Y.; Chen, P.; Wei, F.; Rupprechter, G.; Shen, Y. R.; Somorjai, G. A. *Rev. Sci. Instrum.* **2001**, *72*, 1806.
(18) Yang, M.; Tang, D. C.; Somorjai, G. A. *Rev. Sci. Instrum.* **2003**, *74*, 4554.
(19) Saeys, M.; Reyniers, M.; Marin, G. B.; Neurock, M. *Surf. Sci.* **2002**, *513*, 315.

(20) Su, X.; Shen, Y. R.; Somorjai, G. A. *Chem. Phys. Lett.* **1997**, *280*, 302.
(21) Su, X.; Kung, K. Y.; Lahtinen, J.; Shen, Y. R.; Somorjai, G. A. *J. Mol. Catal. A* **1999**, *141*, 9.
(22) Manner, W. L.; Girolami, G. S.; Nuzzo, R. G. *J. Phys. Chem. B* **1998**, *102*, 10295.
(23) Yang, M.; Chou, K. C.; Somorjai, G. A. *J. Phys. Chem. B* **2003**, *107*, 5267.
(24) Rodriguez, J. A.; Campbell, C. T. *J. Catal.* **1989**, *115*, 500.
(25) Henn, F. C.; Diaz, A. L.; Bussell, M. E.; Hugenschmidt, M. B.; Domagala, M. E.; Campbell, C. T. *J. Phys. Chem.* **1992**, *96*, 5965.
(26) Pettiette-Hall, C. L.; Land, D. P.; McIver, R. T.; Hemminger, J. C. *J. Am. Chem. Soc.* **1991**, *113*, 2755.
(27) Lamont, C. L. A.; Borbach, M.; Martin, R.; Gardner, P.; Jones, T. S.; Conrad, H.; Bradshaw, A. M. *Surf. Sci.* **1997**, *374*, 215.
(28) Rodriguez, J. A.; Campbell, C. T. *J. Phys. Chem.* **1989**, *93*, 826.
(29) Campbell, C. T.; Campbell, J. M.; Dalton, P. J.; Henn, F. C.; Rodriguez, J. A.; Seimanides, S. G. *J. Phys. Chem.* **1989**, *93*, 806.
(30) Koel, B. E.; Blank, D. A.; Carter, E. A. *J. Mol. Catal. A* **1998**, *131*, 39.
(31) Cremer, P. S.; Su, X.; Shen, Y. R.; Somorjai, G. A. *J. Am. Chem. Soc.* **1996**, *118*, 2942.
(32) Cassuto, A.; Kiss, J.; White, J. *Surf. Sci.* **1991**, *255*, 289.
(33) Christmann, K.; Ertl, G.; Pignet, T. *Surf. Sci.* **1976**, *54*, 365.
(34) Pansoy-Hjelvik, M. E.; Schnabel, P.; Hemminger, J. C. *J. Phys. Chem. B* **2000**, *104*, 6554.
(35) Perry, D. A.; Hemminger, J. C. *J. Am. Chem. Soc.* **2000**, *122*, 8079.
(36) Johnstone, R. A. W.; WIlby, A. H.; Entwistle, I. D. *Chem. Rev.* **1985**, *85*, 129.
(37) Felix, A. M.; Heimer, E. P.; Lambros, T. J.; Tzougraki, C.; Meienhofer, J. *J. Org. Chem.* **1978**, *43*, 4194.
(38) Brieger, G.; Nestrick, T. J. *Chem. Rev.* **1974**, *74*, 568.
(39) Viswanatha, V.; Hruby, V. J. *J. Org. Chem.* **1980**, *45*, 2010.
(40) Gowda, D. C.; Abiraj, K. *Lett. Pept. Sci.* **2002**, *9*, 153.
(41) Yang, M.; Somorjai, G. A. *J. Am. Chem. Soc.* **2003**, *125*, 11131.
(42) Hirose, C.; Yamamoto, H.; Akamatsu, N.; Domen, K. *J. Phys. Chem.* **1993**, *97*, 10064.
(43) Newton, M. A.; Campbell, C. T. *Z. Phys. Chem.* **1997**, *198*, 169.
(44) Öfner, H.; Zaera, F. *J. Phys. Chem. B* **1997**, *101*, 396.
(45) Bishop, A. R.; Girolami, G. S.; Nuzzo, R. G. *J. Phys. Chem. B* **2000**, *104*, 754.
(46) Marchenko, O.; Cousty, J. *Phys. Rev. Lett.* **2000**, *84*, 5363.
(47) Firment, L. E.; Somorjai, G. A. *J. Chem. Phys.* **1977**, *66*, 2901.
(48) Manner, W. L.; Bishop, A. R.; Girolami, G. S.; Nuzzo, R. G. *J. Phys. Chem. B* **1998**, *102*, 8816.
(49) Chesters, M. A.; Gardner, P.; McCash, E. M. *Surf. Sci.* **1989**, *209*, 89.
(50) Huang, D.; Chen, Y.; Fichthorn, K. A. *J. Chem. Phys.* **1994**, *101*, 11021.
(51) Janssens, T. V. W.; Zaera, F. *Surf. Sci.* **2002**, *501*, 1.
(52) Ilharco, L. M.; Garcia, A. R.; Hargreaves, E.; Chesters, M. A. *Surf. Sci.* **2000**, *459*, 115.
(53) Fan, J.; Trenary, M. *Langmuir* **1994**, *10*, 3649.
(54) Star, D.; Kikteva, T.; Leach, G. W. *J. Chem. Phys.* **1999**, *111*, 14.
(55) Miranda, P. B.; Pflumio, V.; Saijo, H.; Shen, Y. R. *J. Am. Chem. Soc.* **1998**, *120*, 12092.
(56) Chesters, M. A.; De La Cruz, C.; Gardner, P.; McCash, E. M.; Pudney, P.; Shahid, G.; Sheppard, N. *J. Chem. Soc., Faraday Trans.* **1990**, *86*, 2757.
(57) Zaera, F.; Godbey, D.; Somorjai, G. A. *J. Catal.* **1986**, *101*, 73.
(58) Zaera, F. *Chem. Rev.* **1995**, *95*, 2651.